Perturbations of an anisotropic spacetime: Radiation filled medium

Hyerim Noh
Korea Astronomy Observatory, San 36-1, Whaam-dong, Yusung-gu, Daejon, Korea
(Received 14 July 1995)

We consider the evolution of a perturbed Bianchi type-I model universe filled with a radiation fluid. The background model shows a smooth transition from the shear-dominated early anisotropic universe to the radiation-dominated isotropic one. We have analytic solutions describing the background evolution. We numerically investigate the evolution of perturbations in the metric and the fluid variables through the transition. We consider the wave vector lying in a plane of two principal axes of the background anisotropy. In view of the well-studied case in the isotropic model we adopt the comoving gauge to treat the density perturbation in an ideal fluid. Because of the coupling between different modes in the anisotropic stage, the amplitude of resulting tensor perturbation in the isotropic stage is comparable to the one of scalar perturbation. We present the evolution characterizing the density perturbation and the gravitational waves in some selected parameter space.

PACS number(s): 98.80.Hw, 98.70.Vc

I. INTRODUCTION

In our previous work we presented a general formulation for studying the perturbations in a Bianchi type-I background metric [1]. An application is made to the case where the energy-momentum content is filled with an ideal fluid [2]. In such a model the early shear-dominated anisotropic universe later becomes the matter-dominated isotropic one. In [2] we considered the case where the perturbation wave vector lies in a plane of two principal axes of the background anisotropy. We presented the equations using dimensionless variables, and derived asymptotic solutions in the shear-dominated stage. In the present paper, as a concrete application, we numerically investigate the evolution in the background filled with the radiation fluid. We give the analytic solutions which describe the smooth transition of the background model from the early shear-dominated anisotropic stage to the later radiation-dominated isotropic stage.

In an anisotropic universe, there exist couplings of all three types of modes. In an ideal fluid case with the wave vector in a plane of two principal axes, we have two decoupled sets of equations. In one set the scalar mode is coupled with one polarization state of the gravitational wave and one vector mode; thus, in this case, generally we have a fifth-order differential equation. In the other set, the other polarization state of gravitational wave mode couples with the other remaining vector mode; thus, in general, we have a third-order differential equation. In both sets, the rotation modes work only as sources for other modes. Equations in dimensionless forms are presented in Eqs. (17)–(29) of [2]. Thus, in general, we need the numerical treatment to investigate these perturbation equations. In this paper we *consider* a medium with radiation.

In the Friedman-Lemaitre-Robertson-Walker (FLRW) universe the relevant scales appearing in the perturbation equations are the sound horizon for the scalar mode and the visual horizon for the tensor mode. For the radiation fluid, since $c_s = c/\sqrt{3}$, the sound horizon scale is comparable to the visual horizon scale. Inside the horizon the density contrast ($\delta \equiv \delta\mu/\mu$) of the radiation fluid shows oscillation with constant amplitude [see Eq. (G23) of [1]], whereas inside the horizon the gravitational wave shows oscillating behavior with decaying amplitude [see Eq. (G28) of [1]].

In the FLRW regime, the density perturbation variable in the comoving gauge (CG) shows a similar behavior to the Newtonian one; the perturbed potential and the perturbed velocity variables in the zero-shear gauge (ZSG) show similar behaviors to the corresponding Newtonian ones. Because of the nonvanishing shear in the anisotropic background, we have the uniform-shear (vanishing scalar part of the perturbed shear variable) condition as a gauge-fixing condition; see Sec. III B 1 of [1]. On scales larger than the "sound" horizon, from Tables 2 and 8 of [3] we have

$$\varphi|_{\rm CG} = \text{const in time} = \left(1 - \frac{\dot{a}}{a^2}\int^t a dt\right)^{-1} \varphi|_{\rm ZSG} = \frac{5+3w}{3(1+w)}\varphi|_{\rm ZSG}, \tag{1}$$

where $a(t)$ and $\varphi(\mathbf{x},t)$ are the scale factor and the perturbed potential (related to the perturbed spatial curvature), respectively; $w \equiv p/\mu$ where p and μ are the pressure and the energy density, respectively. An overdot denotes the time derivative based on the background proper time t.

Equation (1) is valid for generally time-varying equations of state with $p = p(\mu)$; in the last step we used $w = \text{const}$ and thus $a \propto t^{2/[3(1+w)]}$. In Eq. (G13) of [1] we showed that $\varphi = \frac{1}{2}C$; $-\varphi$ in the zero-shear gauge corresponds to the perturbed Newtonian gravitational potential. C is a part of the perturbed three space metric defined in Eq. (12) of [1]. From Eq. (B3) of [1] we have $R^{(h)} = -2e^{-2s}C^{|\alpha}{}_{\alpha}$. Thus, C also characterizes the perturbed part of the intrinsic (Ricci) curvature. From Eq. (1) we note that, although C in the zero-shear gauge has the correct Newtonian correspondence, C in the comoving gauge shows simpler behavior; i.e., $C|_{\mathrm{CG}} = \text{const}$ in time for a general equation of state $p = p(\mu)$. In this paper we will investigate the evolution of perturbations in the comoving gauge. The evolution of the perturbed velocity and the potential in the uniform-shear gauge condition will be considered elsewhere.

In Sec. II A we present the background evolution. In Sec. II B the perturbation scales are presented. In Sec. II C we present the perturbed equations in the comoving gauge which describe the coupled evolution of the scalar mode and one polarization state of the gravitational wave. In Sec. II D the perturbed equations for the decoupled set of gravitational wave are presented. In Sec. III A the large scale asymptotic solutions for initial conditions are derived. In Sec. III B we comment on the parameter space which we are considering. In Sec. III C the numerical method for solving the perturbed equations is briefly mentioned. In Sec. III D the numerical results are shown. We will present the temporal evolution of the perturbation variables in a few selected parameter spaces. In Sec. IV the discussion is given. As a unit we set $c \equiv 1$.

II. EQUATIONS

A. Background evolution

We consider a Bianchi type-I model supported by a radiation fluid with $w = \frac{1}{3}$. The background equations are [Eqs. (2)–(4) of [2]]

$$\dot{\mu} + 4\dot{s}\mu = 0, \quad \ddot{s}_\alpha + 3\dot{s}\dot{s}_\alpha = 0, \quad \dot{s}^2 = \frac{8\pi G\mu}{3} + \frac{1}{6}\sum_\alpha \dot{s}_\alpha^2, \tag{2}$$

where $\sum_{\alpha=1}^{3} s_\alpha = 0$, $s_\alpha = s_\alpha(t)$, $s = s(t)$. Thus, $\dot{s}_\alpha \propto e^{-3s}$ and $\mu \propto e^{-4s}$.

Using η as a time variable ($d\eta \equiv a^{-1}dt$, $a \equiv e^s$) the solutions are derived in Eq. (A5) of [2]:

$$e^s = \left(\frac{8\pi G}{3}\mu e^{4s}\right)^{1/2}\sqrt{\eta\,(\eta + 2\eta_s)}, \quad e^{s_\alpha} = \left(\frac{\eta}{\eta + 2\eta_s}\right)^{S_\alpha/2}, \tag{3}$$

where

$$\eta_s \equiv \frac{3}{2}\frac{\sqrt{\frac{1}{6}\sum_\alpha \dot{s}_\alpha^2}}{4\pi G\mu e^s}, \quad S_\alpha \equiv \frac{\dot{s}_\alpha}{\sqrt{\frac{1}{6}\sum_\beta \dot{s}_\beta^2}}. \tag{4}$$

Since $\sum_\alpha S_\alpha = 0$ and $\sum_\alpha S_\alpha^2 = 6$, S_α can be represented by a parameter u; see Eq. (31) of [2]. We normalized $a(\eta)$ as $a = 0$ at $\eta = 0$. We also set $8\pi G\mu e^{4s} = \eta_s^{-2}$, thus normalizing the scale factor as $a(\eta_s) \equiv 1$. η_s indicates the transition time from the shear-dominated into the radiation-dominated era. In the limiting cases of the shear-dominated era (SDE) and the radiation-dominated era (RDE) we have

$$\text{SDE}: \quad \eta \ll \eta_s \left(\eta \propto t^{2/3}\right): \quad e^s \propto \eta^{1/2} \propto t^{1/3}, \quad e^{s_\alpha} \propto \eta^{S_\alpha/2} \propto t^{S_\alpha/3}; \tag{5}$$

$$\text{RDE}: \quad \eta \gg \eta_s \left(\eta \propto t^{1/2}\right): \quad e^s \propto \eta \propto t^{1/2}, \quad e^{s_\alpha} \to 1. \tag{6}$$

From Eq. (3) we have

$$\frac{\eta}{\eta_s} = \sqrt{1 + 3e^{2s}} - 1. \tag{7}$$

Some trends of the background evolution are presented in Fig. 1.

B. Perturbation scales

The perturbed equations will be analyzed in Fourier space. Thus, the equations turn into ordinary coupled differential equations. Since the Bianchi type-I model is spatially flat, we can decompose the spatial dependence of the perturbed variables using a wave vector $\mathbf{k}$ as $A(\mathbf{x},t) \propto \int A_{\mathbf{k}}(t)e^{i\mathbf{k}\cdot\mathbf{x}}d^3k$, etc. To linear order, perturbations with different wave vectors do not mix together. Thus, we can single out a particular wave vector $\mathbf{k}$ and consider the equation for $A_{\mathbf{k}}(t)$. Since the same form of equations is valid for the Fourier amplitude $A_{\mathbf{k}}(t)$ with the spatial derivative which changes into the corresponding combination of wave vectors, without causing any

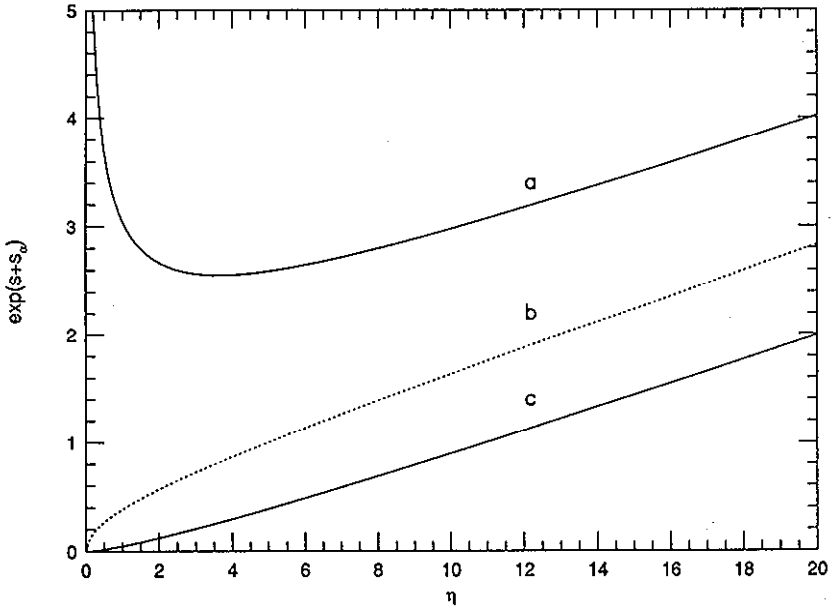

FIG. 1. Plot of $e^{s+s_\alpha}(\eta)$. (a), (b), and (c) represent the evolution of three different directions for $S_\alpha = (-\sqrt{3}, 0, \sqrt{3})$. In the early stage, the background evolves differently in different directions, and is thus anisotropic. But they evolve like the FLRW universe at large η. The transition occurs near $\eta_s = 5$.

confusion, we often neglect the subindex **k** to indicate the Fourier amplitude.

The size and the direction (with respect to the principal axes of the background anisotropy) of the perturbations can be characterized by the wave vector k_α. We align the coordinate so that $\hat{x}^1 = (1,0,0)$, $\hat{x}^2$, and $\hat{x}^3$ are three orthogonal directions of the principal axes of the background anisotropy. In this paper we consider the situation where the wave vector k_α lies in a plane of two principal axes, thus $k_\alpha = (0, k_2, k_3)$. The index of k^α vector is raised by using $\gamma^{\alpha\beta}$ as a metric; see Eqs. (1) and (2) of [1]. We have

$$k^2 k_2 = \gamma^{22}(k_2)^2 = e^{-2s_2}(k_2)^2 = \left(\frac{\eta}{\eta+2\eta_s}\right)^{-S_2}(k_2)^2,$$
$$k^3 k_3 = \left(\frac{\eta}{\eta+2\eta_s}\right)^{-S_3}(k_3)^2. \tag{8}$$

We introduce

$$r \equiv \frac{k_2}{k_3}, \quad \Delta \equiv \gamma^{\alpha\beta}\partial_\alpha\partial_\beta \equiv \nabla^{(3)\alpha}\partial_\alpha. \tag{9}$$

In Fourier space we have $\Delta = -\gamma^{\alpha\beta}k_\alpha k_\beta = -k^\alpha k_\alpha$ which becomes $\Delta = -(k^2k_2 + k^3k_3)$ in our alignment of the wave vector. Using $k \equiv \sqrt{k^\alpha k_\alpha}$, we have

$$\begin{aligned}\bar{\Delta} &\equiv \frac{\Delta}{(a\dot{s})^2} \\ &= -\left(\frac{k}{a\dot{s}}\right)^2 = -(k\eta)^2\left(\frac{\eta+2\eta_s}{\eta+\eta_s}\right)^2 \\ &= -\left(k_3\eta\right)^2\left(\frac{\eta+2\eta_s}{\eta+\eta_s}\right)^2\left[\left(\frac{\eta}{\eta+2\eta_s}\right)^{-S_3}\right. \\ &\quad \left.+\left(\frac{\eta}{\eta+2\eta_s}\right)^{-S_2} r^2\right].\end{aligned} \tag{10}$$

The horizon crossing epoch of a given scale k, $\eta_H(k)$, is *defined* as

$$1 \equiv \sqrt{-\bar{\Delta}|_H} = \left.\frac{k}{a\dot{s}}\right|_H. \tag{11}$$

From this relation we can express k_3 in terms of η_H and r as

$$k_3 = \frac{\eta_H+\eta_s}{\eta_H+2\eta_s}\frac{1}{\eta_H}\left[\left(\frac{\eta_H}{\eta_H+2\eta_s}\right)^{-S_3}\right. \\ \left.+\left(\frac{\eta_H}{\eta_H+2\eta_s}\right)^{-S_2} r^2\right]^{-1/2}. \tag{12}$$

The wave propagation vectors k_2 and k_3 will be specified in terms of r and η_H. The parameters r and η_H characterize the direction and the size of the wave vector, respectively.

C. Perturbed equations in the comoving gauge

The set of perturbation equations describing the set including the scalar mode is presented in Eqs. (17)–(26) of [2]. The equation for the rotation mode Q_v is independent of other equations. However, the rotation mode can work as a source for other modes. In the following we *ignore* the contribution from the rotation mode. By irrotational condition we mean $Q_v = 0$. However, the scalar and the tensor modes can generate the B_v term; see Eq. (26) of [2].

In the comoving gauge, we let

$$\bar{Q} \equiv 0. \tag{13}$$

In the following, we present the fundamental equations for general $w = \text{const}$. From Eqs. (18), (19), (20), (24), and (26) of [2], we have

$$\delta\bar{K} = \frac{\delta' - 3w\delta}{1+w}, \tag{14}$$

$$\delta\bar{K}' = -\left(2 + \frac{\ddot{s}}{\dot{s}^2} - \frac{\Delta'}{\Delta}\right)\delta\bar{K} + \left[\bar{\Delta} - 3 + \sum_\alpha s_\alpha'^2 - \frac{3}{4}\frac{\Delta'^2}{\Delta^2}\right]\frac{w}{1+w}\delta + \frac{1+3w}{1+w}\frac{4\pi G\mu}{\dot{s}^2}\delta$$
$$-\frac{9}{8}\frac{\Delta'^2}{\Delta^2}C + \left(s_1' - \frac{\Delta'}{4\Delta}\right)\left(4G' - 3\frac{\Delta'}{\Delta}G\right) + 4\left(s_2' - s_3'\right)^2\frac{k^2k_2k^3k_3}{\Delta^2}\left(-\frac{w}{1+w}\delta - \frac{3}{2}C + G\right), \tag{15}$$

$$G'' = -\left(3 + \frac{\ddot{s}}{\dot{s}^2}\right)G' + \bar{\Delta}G + \left(s_1' - \frac{\Delta'}{4\Delta}\right)\frac{1-w}{1+w}\delta' - 2\left(s_2' - s_3'\right)^2\frac{k^2k_2k^3k_3}{\Delta^2}\left(-\frac{w}{1+w}\delta - \frac{3}{2}C + G\right), \tag{16}$$

where a prime denotes the time derivative with respect to s, $' \equiv \frac{\partial}{\partial s}$. From Eqs. (19), (21), (22), and (26) of [2] we have

$$C = -\left[2\bar{\Delta} - \frac{9\Delta'^2}{8\Delta^2} - 6(s_2' - s_3')^2\frac{k^2k_2k^3k_3}{\Delta^2}\right]^{-1}\left\{\left(4 + \frac{\Delta'}{\Delta}\right)\delta\bar{K}\right.$$
$$+\frac{16\pi G\mu}{\dot{s}^2}\delta + \left[2\sum_\alpha s_\alpha'^2 - \frac{3}{4}\frac{\Delta'^2}{\Delta^2} - 4(s_2' - s_3')^2\frac{k^2k_2k^3k_3}{\Delta^2}\right]\frac{w}{1+w}\delta$$
$$\left.+4\left(s_1' - \frac{\Delta'}{4\Delta}\right)G' + 4(s_2' - s_3')^2\frac{k^2k_2k^3k_3}{\Delta^2}G - 3\frac{\Delta'}{\Delta}\left(s_1' - \frac{\Delta'}{4\Delta}\right)G\right\}. \tag{17}$$

Equations (14)–(17) describe the coupled evolution of the scalar mode (characterized by δ or C) and one polarization state of the gravitational wave (G). These equations can be combined into a fourth-order differential equation for δ or G.

A combination of the wave vector $k^2k_2k^3k_3/\Delta^2$ appears in several places in our perturbed set of equations [Eqs. (14)–(18)]. We present the evolution of this quantity in Fig. 2. As r increases, the slope change of $k^2k_2k^3k_3/\Delta^2$ occurs at an earlier time. Since $S_3 > S_2$, in the early enough time we have $k^3k_3 \gg k^2k_2$ for any r ($k_3 \neq 0$). Thus, in the early time, the wave vector is in the $\hat{k}_3$ direction effectively. As the background approaches the FLRW regime, $\sqrt{k^2k_2/k^3k_3}$ approaches r. Thus, for large values of r, the transition of the effective wave direction from the $\hat{k}_3$ direction into the $\hat{k}_\alpha$ direction with $k_2/k_3 = r$ will occur earlier. For all cases with different values of r, as s becomes large, $k^2k_2k^3k_3/\Delta^2$ approaches $r^2/(1+r^2)^2$. Later we will see that this term causes the perturbed variables (δ, C, G, etc.) to change their slopes at an earlier time as r increases; compare with Figs. 3(a)–3(c).

D. Decoupled gravitational wave mode

A set of equations for the decoupled gravitational wave mode is given in Eqs. (27)–(29) of [2]. The decoupled gravitational wave is determined by a second-order differential equation with $\bar{Q}_v$ as a source. We *ignore* $\bar{Q}_v$; thus, $\bar{Q}_v \equiv 0$. However, $\bar{B}_v$ does not vanish, and we have

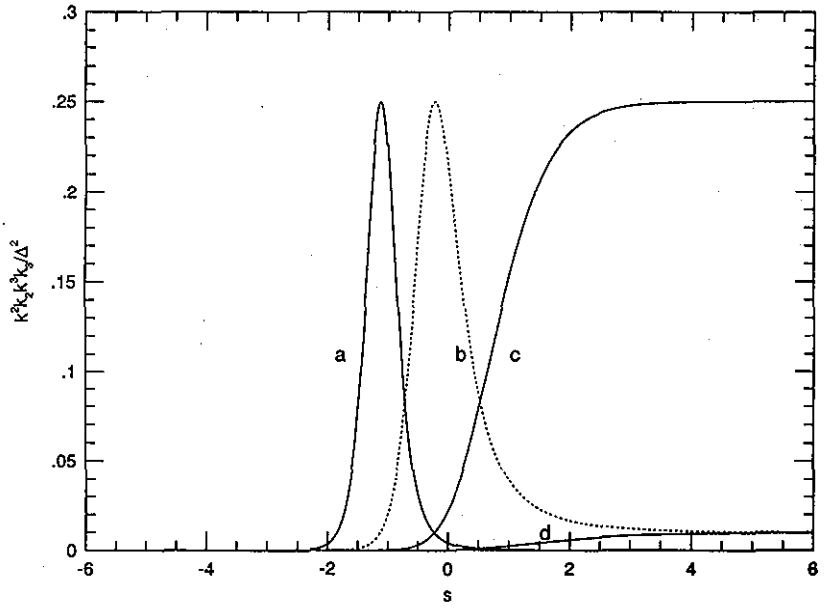

FIG. 2. The time evolution of $k^2k_2k^3k_3/\Delta^2$ for $r = 100$ (a), 10 (b), 1 (c), and 0.1 (d). We consider $S_\alpha = (0, -\sqrt{3}, \sqrt{3})$.

$$\bar{G}'' + \left[3 + \frac{\ddot{s}}{\dot{s}^2} + 2(s_1' - s_2') + 2(s_2' - s_3')\frac{k^2k_2}{\Delta}\right]\bar{G}' + \left[-\bar{\Delta} + 4(s_2' - s_3')(s_1' - s_2')\frac{k^2k_2}{\Delta} + 4(s_2' - s_3')^2\frac{k^2k_2k^3k_3}{\Delta^2}\right]\bar{G} = 0. \quad (18)$$

This equation describes the evolution of the decoupled gravitational wave ($\bar{G}$).

III. EVOLUTIONS

A. Initial conditions

In the numerical study we will consider Eqs. (14)–(17) as differential equations for δ and G. As the initial condition we can use the large scale asymptotic solutions of the perturbed variables in the shear-dominated stage which were derived in Eqs. (43), (44), and (47) of [2]. For $w = \frac{1}{3}$ we have

$$\delta(\mathbf{x},t) \equiv \frac{4}{3}a_1(\mathbf{x})e^{-2s} + \frac{4}{3}\left[1 + \frac{1}{4(2-S_3)(5-S_3)}\bar{\Delta}\right]a_2(\mathbf{x}) + \frac{4}{3}\bar{\Delta}\left[1 + \frac{(7-2S_3)}{24(2-S_3)^2(5-2S_3)}\bar{\Delta}\right]a_3(\mathbf{x}) + \frac{4}{3}s\bar{\Delta}a_4(\mathbf{x}), \quad (19)$$

$$C(\mathbf{x},t) = -\frac{1}{3}(2-S_3)a_1e^{-2s} - \frac{2-S_3}{3(5-S_3)}a_2 - \left[2(2-S_3)(3-S_3) + \frac{5-S_3}{6(2-S_3)}\bar{\Delta}\right]a_3 - [5 - 2S_3 + 2(2-S_3)(3-S_3)s]a_4, \quad (20)$$

$$G(\mathbf{x},t) = -\frac{1}{6}(S_1-S_2)a_1e^{-2s} + \frac{2}{3}\frac{1}{(S_1-S_2)}\left\{-1 + \frac{1}{2(5-S_3)}\left[S_3(2-S_3) - \frac{1}{4}\bar{\Delta}\right]\right\}a_2 + \left\{-3\frac{S_3}{S_1-S_2}(2-S_3)(3-S_3) + \frac{3}{8(S_1-S_2)(2-S_3)}\left[8 - 7S_3 + \frac{1}{3}\left(-8 + 3S_3 + 2S_3^2\right)\right]\bar{\Delta}\right\}a_3 + \frac{1}{2}\frac{1}{S_1-S_2}[8(3-S_3) + S_3(-27 + 10S_3) - 6S_3(2-S_3)(3-S_3)s]a_4, \quad (21)$$

where $a_1(\mathbf{x})$, $a_2(\mathbf{x})$, $a_3(\mathbf{x})$, and $a_4(\mathbf{x})$ are four integration constants. $a_i(\mathbf{x})$ determines the initial amplitudes of four different modes. Unless we have the physical mechanism which can determine the relation between the amplitudes each amplitude can be given arbitrarily as the initial condition.

For the decoupled gravitational wave $\bar{G}$, the large scale asymptotic solutions are presented in Eq. (68) of [2]. We ignored the rotation mode and have

$$\bar{G}(\mathbf{x},t) = g_1(\mathbf{x})e^{-2(S_1-S_2)s} + g_2(\mathbf{x}), \quad (22)$$

where $g_1(\mathbf{x})$ and $g_2(\mathbf{x})$ are constant coefficients of the second-order differential equation [Eq. (18)].

B. Parameter space

In order to specify the scale and the configuration of the perturbation, we use the following quantities as parameters.

(1) The direction of the wave vector relative to the principal axes of the background anisotropy is specified by $r(\equiv k_2/k_3)$.

(2) The size of perturbation is specified by using η_H which indicates the horizon-crossing epoch for a given scale k_3 and r.

(3) The rate of background anisotropy is determined by S_α; as we mentioned below Eq. (4), S_α can be represented by a parameter u.

In Sec. II E of [2] we made brief comments on some special situations of the background anisotropy and the perturbations. The numerical results using this parameter space with some discussion will be given in Sec. III D.

C. Numerical methods

The scalar mode is characterized by variables δ and C. The tensor mode is characterized by a variable G and a decoupled $\bar{G}$. We ignore the vector mode. In this

paper we take the (spatial) C gauge and the (temporal) comoving gauge. This set of gauge conditions completely fixes all gauge modes. Thus, under this set of gauge conditions the variables are gauge free and consequently each variable has a unique corresponding gauge-invariant combination; see Sec. III C of [1].

The evolutions of δ, C, and G can be obtained by solving Eqs. (14)–(17) numerically. The evolution of $\bar{G}$ can be obtained by solving Eq. (18). The exact behavior of some useful quantities appearing as coefficients in the equations is presented in the Appendix. For given values of the parameters r, η_H, and u, we used the Runge-Kutta method to integrate the set of differential equations from the initial stage ($= s_i$) to the final stage ($= s_f$). We typically set $s_i = -10$, $s_f = 10$, and $s_s = 0$; s_s is the value of s at the transition from the shear-dominated era into the radiation-dominated era, i.e., at η_s. However, for large values of r, we need much smaller values of s_i (much earlier initial stage), since our asymptotic solutions are valid on the condition that $\sqrt{(k^2k_2)/(k^3k_3)} = (e^s)^{S_3-S_2}r \ll 1$; see Eq. (36) of [2]. We typically divided the time duration into 5000 steps for which the results almost do not change ($\lesssim 1\%$) with varying the step size.

For the initial amplitude, we typically set $a_i = 10^{-10}$ ($i = 1, 2, 3, 4$). Since this value is arbitrary, only the relative scale is important. As initial conditions, we need the values for δ, δK, G, G' at s_i, and usually choose the a_3 mode of the asymptotic solutions (in Sec. III A) which show the growing behavior together with a_4 mode; the a_3 mode shows the same behavior as the growing mode in the FLRW situation [see Eqs. (49)–(54) of [2]]. Unless otherwise mentioned, we assume that the horizon crossing occurs much later than the transition time s_s; we typically set $s_H = 15$, where s_H is the value of s at the horizon crossing η_H.

D. Results

In Fig. 3(a) we show the evolution of δ for the a_3 mode for different values of r. In the following, unless

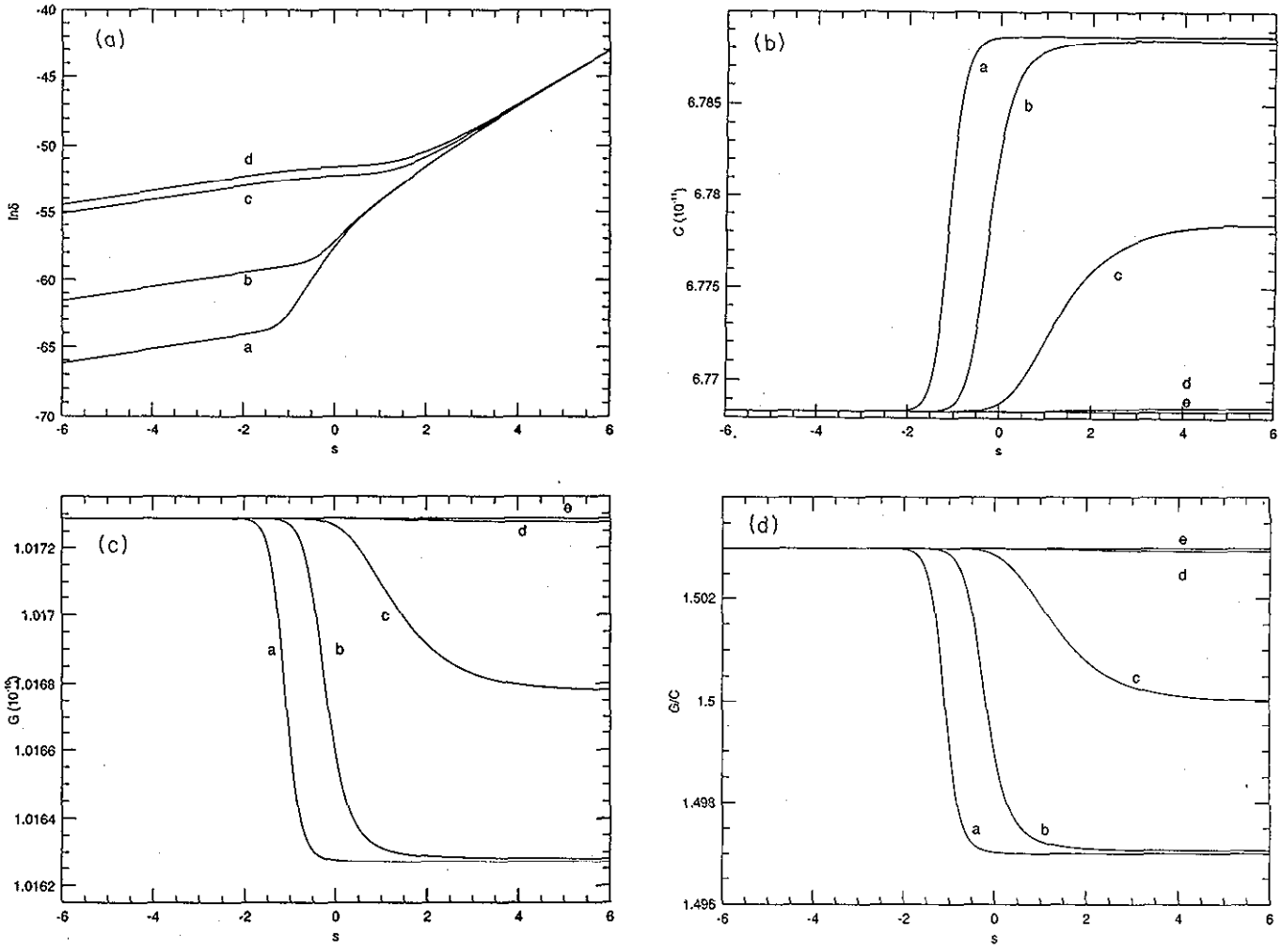

FIG. 3. (a) $\ln\delta(s)$ for $r = 0$, 0.01, 0.1 (d), 1 (c), 10 (b), 100 (a). We take one of the growing modes a_3 as the initial condition. We consider $S_\alpha = (0, -\sqrt{3}, \sqrt{3})$. (b) $C(s)$ in units of 10^{-11} for $r = 0$, 0.01 (e), 0.1 (d), 1 (c), 10 (b), 100 (a), and $S_\alpha = (0, -\sqrt{3}, \sqrt{3})$. The a_3 mode is considered. (c) $G(s)$ in units of 10^{-10} for $r = 0$, 0.01 (e), 0.1 (d), 1 (c), 10 (b), 100 (a), and $S_\alpha = (0, -\sqrt{3}, \sqrt{3})$. The a_3 mode is considered. (d) The ratio of $G(s)$ to $C(s)$ for $r = 0$, 0.01 (e), 0.1 (d), 1 (c), 10 (b), 100 (a), and $S_\alpha = (0, -\sqrt{3}, \sqrt{3})$. The a_3 mode is considered.

otherwise mentioned we will take the a_3 mode as the initial condition. For Figs. 3(a)–3(d) we considered $S_\alpha = (0, -\sqrt{3}, \sqrt{3})$.

As introduced in Sec. II B, r determines the direction of the perturbation wave vector; as r becomes large, the direction of the perturbation wave vector is close to $\hat{x}^2$-axis. For a case with $r = 0$, the wave vector always lies in the $\hat{x}^3$ direction with $k_\alpha = (0, 0, k_3)$. It is noticeable that δ changes its growth rate near $s = 0$ where the transition from the shear-dominated era into the radiation-dominated era occurs. Especially, in the case of using the a_3 mode as the initial condition, the δ evolves like $e^{4-2S_\alpha(\mathbf{k}_{\rm eff})}$ in the shear-dominated era, where $S_\alpha(\mathbf{k}_{\rm eff})$ indicates the S_α with the effective wave vector $\mathbf{k}_{\rm eff} = (0, \sqrt{k^2 k_2}, \sqrt{k^3 k_3})$. At large values of s, δ evolves like the FLRW universe in the radiation-dominated era ($\delta \propto e^{2s} \propto \eta^2 \propto t$). The evolution of the perturbation in the early stage is affected by the background anisotropy. The growth rate of the density perturbation has a directional dependence, i.e., depends on r.

We see that as r increases, another change in the growth rate appears between the shear-dominated era and the FLRW regime. For large r, the effective wave vector of the perturbation, $\mathbf{k}_{\rm eff} = (0, \sqrt{k^2 k_2}, \sqrt{k^3 k_3})$, changes from $(0, 0, \sqrt{k^3 k_3})$ into $(0, r\sqrt{k^3 k_3}, \sqrt{k^3 k_3})$. Thus, for $S_3 > S_2$ and large r, $\hat{\mathbf{k}}_{\rm eff}$ effectively changes from the $\hat{x}^3$ into the $\hat{x}^2$ direction. The perturbations will be affected by the evolution of the background anisotropy. For example, using the a_3 mode, the result in Fig. 3(a) shows that for large r, δ actually evolves like $\delta \propto e^{4-2S_2}$ in some stage between the initial stage and the FLRW stage. As r increases, the slope change of variables occurs at an earlier time. This fact can be explained by the shift of the slope change in $k^2 k_2 k^3 k_3/\Delta^2$ in the earlier time as r increases as shown in Fig. 2. The dependence of initial values of $\ln\delta$ on r does not have a physical meaning. The amplitude depends on our chosen value of a_3 and r [see Eqs. (19) and (10)], whereas the initial values for the a_3 modes of C and G in the large scale limit do not depend on r [see Eqs. (20) and (21)]. The convergence of $\ln\delta$ for different r in the FLRW regime occurs because we plot δ in logarithemic scale.

We show the evolution of C and G for different value of r in Figs. 3(b) and 3(c), respectively. As in the case of δ, C and G show the change in the growth rate near the transition time s_s, and evolve like the FLRW universe as s increases. Again, these changes in the growth rate occur at an earlier time as r increases. For small r, C and G remain constant for the whole period. For $s \gg s_s$, C and G evolve like the FLRW universe where they remain constant. Even in the shear-dominated era, and thus $s \ll s_s$, C and G remain constant; see Eqs. (20) and (21). The evolution of ratio between C and G for different r is shown in Fig. 3(d). Notice that the values of G is comparable to that of C for different values of r. A similar result was also obtained in [4]; in [4], the uniform-curvature gauge together with the C-gauge condition was used (see Sec. III B of [2]). C and G characterize the amplitudes of the scalar and the tensor perturbations, respectively. Therefore, Fig. 3(d) shows that in the anisotropic universe the tensor perturbation is correlated with the scalar perturbation, while they are independent in the isotropic universe. Such a correlation is reflected in the asymptotic solutions in the shear-dominated era presented in Eqs. (19)–(21). Thus, as the perturbation goes through the anisotropic phase, the resulting amplitude of the tensor mode in the later isotropic phase is comparable to the one of the scalar mode.

As explained in Sec. II E of [2] we have the following cases which representatively cover the whole parameter space (without losing generality we consider $S_3 \geq S_2$):

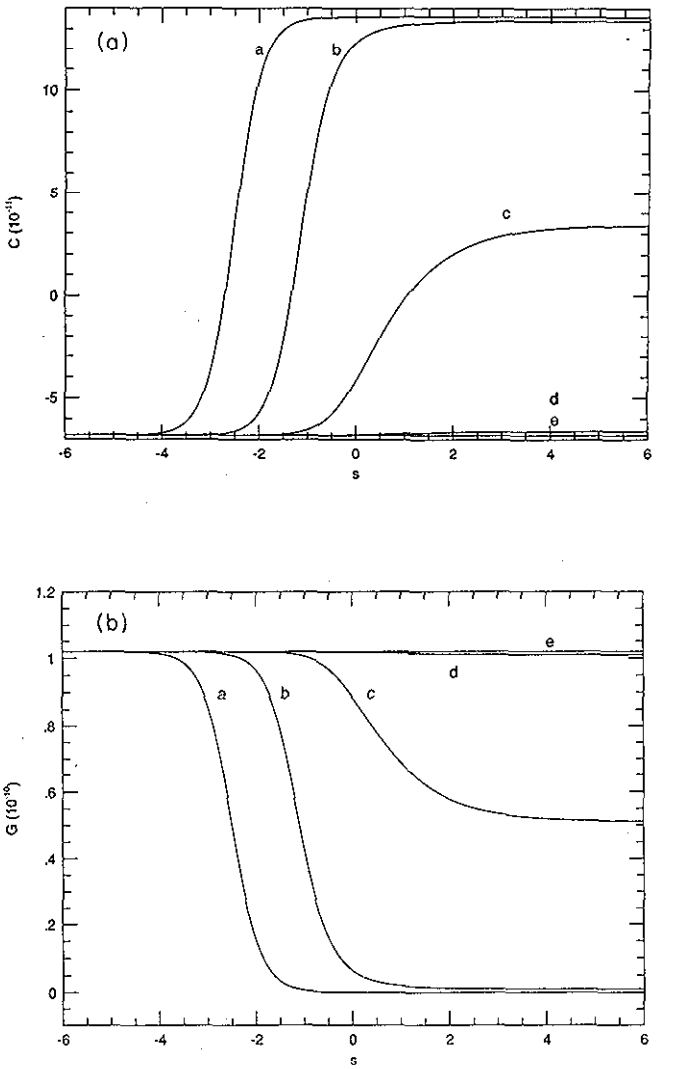

FIG. 4. (a) $C(s)$ in units of 10^{-11} using the background model with $S_\alpha = (-\sqrt{3},\ 0,\ \sqrt{3})$. We consider $r = 0$, 0.01 (e), 0.1 (d), 1 (c), 10 (b), 100 (a). The slope change occurs at an earlier time as r increases. (b) $G(s)$ in units of 10^{-10} using the background model with $S_\alpha = (-\sqrt{3},\ 0,\ \sqrt{3})$. We consider $r = 0$, 0.01 (e), 0.1 (d), 1 (c), 10 (b), 100 (a). The slope change occurs at an earlier time as r increases.

case A1:	$S_\alpha = (0, -\sqrt{3}, \sqrt{3})$	[Figs. 3(a)–3(d)] ;
case A2:	$S_\alpha = (-\sqrt{3}, 0, \sqrt{3})$	[Figs. 4(a), 4(b)] ;
case A3:	$S_\alpha = (\sqrt{3}, -\sqrt{3}, 0)$	[Figs. 5(a), 5(b)] ;
case B1:	$S_\alpha = (1, -2, 1)$	[Figs. 6(a), 6(b)] ;
case B2:	$S_\alpha = (-2, 1, 1)$	[Fig. 7] ;
case C1:	$S_\alpha = (2, -1, -1)$	[Fig. 7] ;
case C2:	$S_\alpha = (-1, -1, 2)$	[Figs. 8(a)–8(c)] .

The cases of $S_\alpha = (1, 1, -2)$ and $(-1, 2, -1)$ are covered by exchanging S_2 with S_3 in cases B1 and C2, respectively, considering a complete coverage in the parameter r; the cases with $S_2 < S_3$ are similarly covered.

For cases A1–A3, we have the system with maximally different background anisotropies in different directions. The evolutions in case A1 are presented in Figs. 3(a)–3(d). We show the evolution of C, and G for case A2 in Figs. 4(a), 4(b), and case A3 in Figs. 5(a), 5(b), using various values of r. Because of the coupling, the behavior of a variable can be derived as a linear combination of other variable(s). However, we may regard C and G as characterizing the evolution of the scalar and tensor

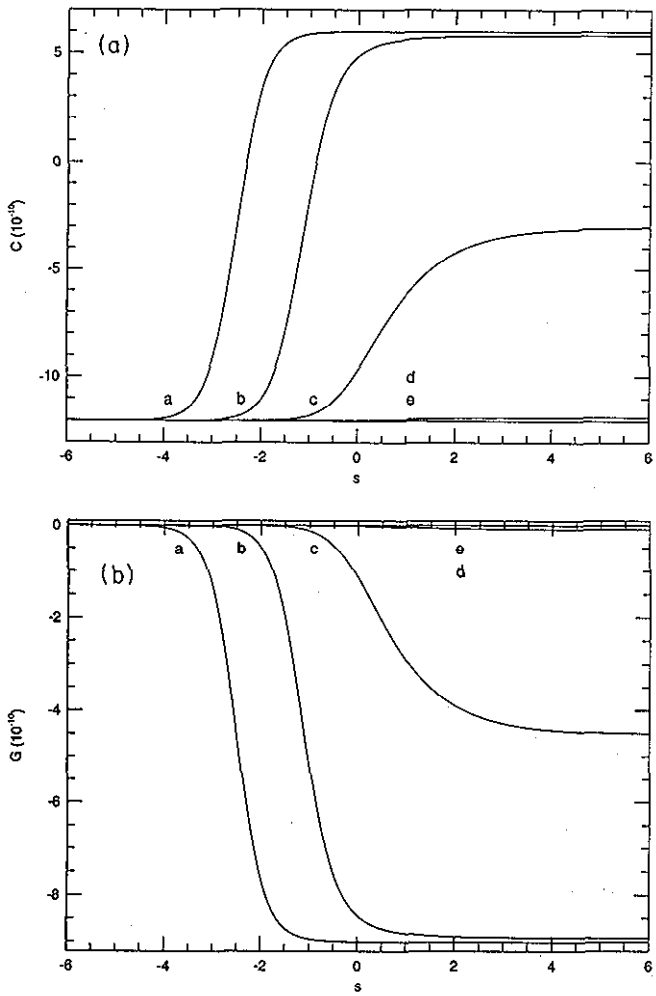

FIG. 5. (a) $C(s)$ in units of 10^{-10} using the background model with $S_\alpha = (\sqrt{3}, -\sqrt{3}, 0)$. We consider $r = 0$, 0.01 (e), 0.1 (d), 1 (c), 10 (b), 100 (a). The slope change occurs at an earlier time as r increases. (b) $G(s)$ in units of 10^{-10} using the background model with $S_\alpha = (\sqrt{3}, -\sqrt{3}, 0)$. We consider $r = 0$, 0.01 (e), 0.1 (d), 1 (c), 10 (b), 100 (a). The case with $r = 0$, 0.01 (e) remains almost constant for all time. The slope change occurs at an earlier time as r increases.

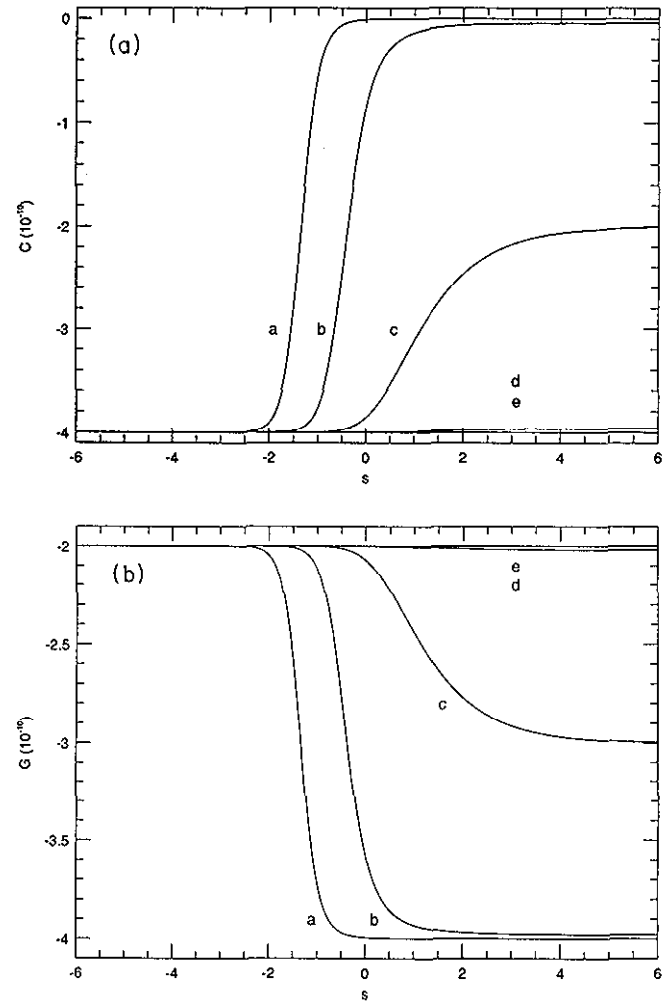

FIG. 6. (a) $C(s)$ in units of 10^{-10} using the background model with $S_\alpha = (1, -2, 1)$. We consider $r = 0$, 0.01 (e), 0.1 (d), 1 (c), 10 (b), 100 (a). The case with $r = 0$, 0.01 (e) remains almost constant for all time. The slope change occurs at an earlier time as r increases. (b) $G(s)$ in units of 10^{-10} using the background model with $S_\alpha = (1, -2, 1)$. We consider $r = 0$, 0.01 (e), 0.1 (d), 1 (c), 10 (b), 100 (a). The case with $r = 0$, 0.01 (e) remains almost constant for all time. The slope change occurs at an earlier time as r increases.

modes, respectively. In the FLRW limit C and G are decoupled and the growing modes of both variables are conserved. We find that for $r = 0$, δ in case A2 is consistent with that in case A1. This must be the case because for $r = 0$ the wave vector lies in the $\hat{x}^3$ direction and the S_3's for cases A1 and A2 coincide with each other.

Figures 6(a), 6(b) show the evolutions of C and G for case B1 in which the background is axisymmetric with respect to the $\hat{x}^2$ axis ($S_1 = S_3$). For cases B2 and C1, the background is axisymmetric with respect to the $\hat{x}^1$ axis ($S_2 = S_3$). In this case, the perturbed variables are independent of r. The variables C and G for cases B2 and C1 remain constant for the whole period.

In Fig. 7, we compare the evolution of δ for cases A1, B2, and C1. Figure 7 shows that in the shear-dominated era the evolution of the perturbation is determined by the property of the background anisotropy. The perturbed variables show different behavior depending on the background anisotropy in the shear-dominated era. At $s \ll s_s$, δ evolves like e^{4-2S_3}, because the wave vector effectively lies in the $\hat{x}^3$ direction. But, at $s \gg s_s$, the perturbations evolve like the FLRW universe.

In Figs. 8(a)–8(c), we present case C2 in which the background model is axisymmetric with respect to the $\hat{x}^3$ axis ($S_1 = S_2$). In this case, the different initial condition was taken. As initial conditions we took the constant mode for G and the a_3 mode for other variables; see Sec. III A2 of [2]. After the transition time, δ first decays and then grows. Both of these decaying ($\propto e^{-s}$) and growing ($\propto e^{2s}$) behaviors are consistent with the FLRW evolution. This behavior occurs at earlier time as r becomes larger. Such behavior may occur because the initial conditions we chose correspond to a mixture of the growing and decaying modes in the FLRW limit.

So far, we considered the large scale perturbation; thus, the horizon crossing occurs much later than the transition time from the shear-dominated into the radiation-dominated era. In Figs. 9(a)–9(c), we present the evolu-

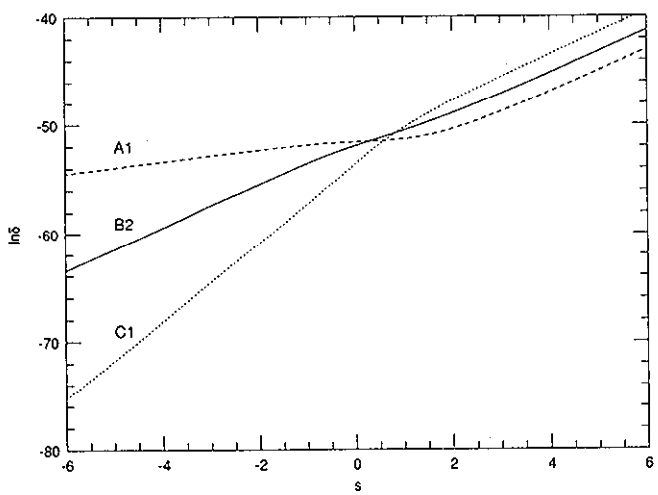

FIG. 7. $\ln\delta(s)$ for three cases: (A1) $S_\alpha = (0, -\sqrt{3}, \sqrt{3})$, (B2) $S_\alpha = (-2, 1, 1)$, (C1) $S_\alpha = (2, -1, -1)$. We consider $r = 0$ and the a_3 mode.

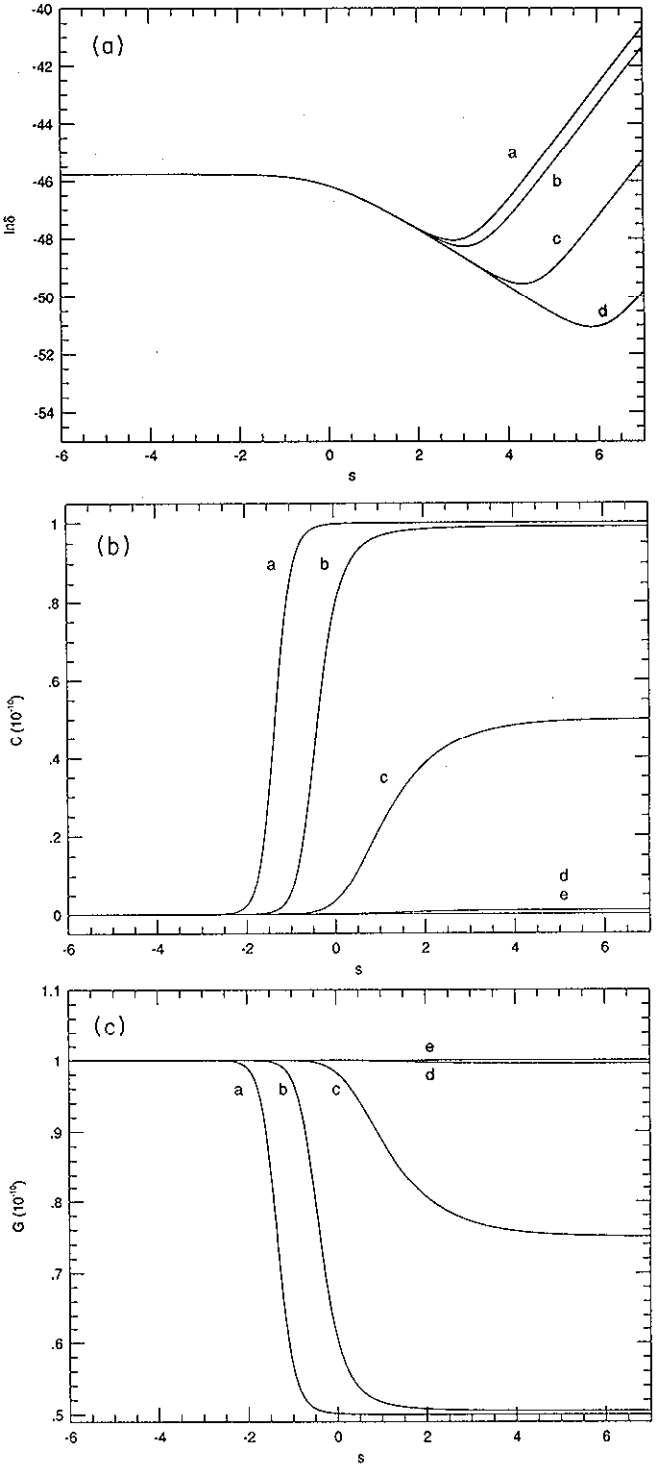

FIG. 8. (a) $\ln\delta(s)$ using the background model with $S_\alpha = (-1, -1, 2)$ in which the model is axisymmetric with respect to the $\hat{x}^3$ axis. We consider $r = 0$, 0.01 (d), 0.1 (c), 1 (b), 10, 100 (a), and consider the a_3 mode. (b) $C(s)$ in units of 10^{-10} using the background model with $S_\alpha = (-1, -1, 2)$. The a_3 mode is considered. We consider $r = 0$, 0.01 (e), 0.1 (d), 1 (c), 10 (b), 100 (a). The case with $r = 0$, 0.01 (e) remains almost constant for all time. The slope change occurs at an earlier time as r increases. (c) $G(s)$ in units of 10^{-10} using the background model with $S_\alpha = (-1, -1, 2)$. The a_3 mode is considered. We consider $r = 0$, 0.01 (e), 0.1 (d), 1 (c), 10 (b), 100 (a). The slope change occurs at an earlier time as r increases.

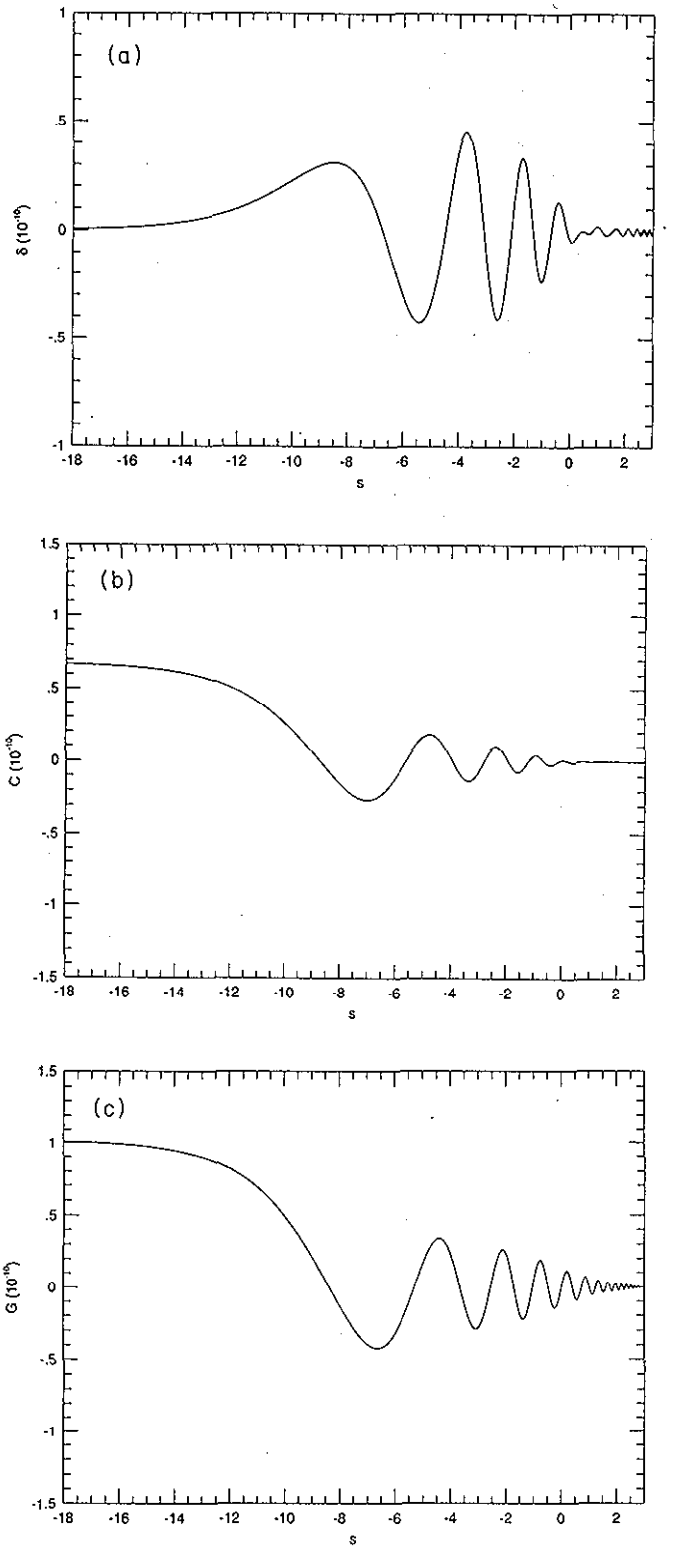

FIG. 9. (a) The evolution of $\delta(s)$ in units of 10^{-10} using the case where the horizon crossing occurs earlier than the transition time s_s. The horizon crossing occurs at $s_H = -7.4$. We consider $r = 0.01$ and the a_3 mode. After the horizon crossing, δ starts to oscillate. In FLRW limit, δ oscillates with constant amplitude. (b) $C(s)$ in units of 10^{-10} using the case where the horizon crossing occurs at $s_H = -7.4$. We consider $r = 0.01$ and the a_3 mode. (c) $G(s)$ in units of 10^{-10} using the case where the horizon crossing occurs at $s_H = -7.4$. We consider $r = 0.01$ and the a_3 mode.

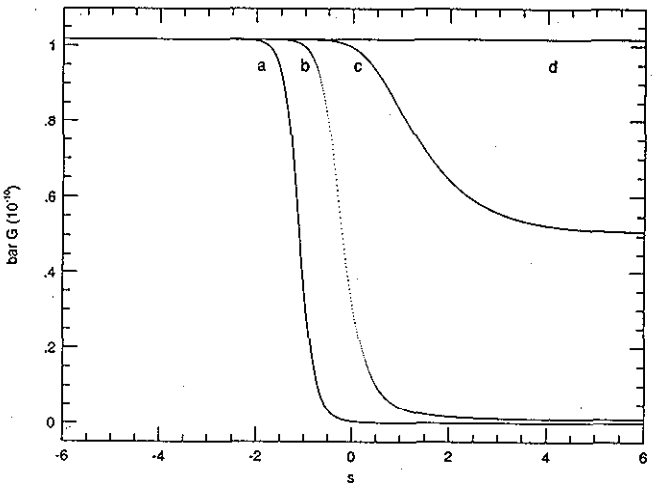

FIG. 10. The evolution of the decoupled gravitational wave $\bar{G}$ in units of 10^{-10} for $r = 0$ (d), 1 (c), 10 (b), 100 (a), using g_2 mode as an initial condition with $g_2 = 10^{-10}$. We consider $S_\alpha = (0, -\sqrt{3}, \sqrt{3})$.

tion of perturbation variables in the case where the horizon crossing occurs much earlier than the transition time s_s. All variables show an oscillation after the horizon crossing. δ starts to oscillate after the horizon crossing. After the transition time s_s, the oscillation amplitude of δ becomes constant which is consistent with the behavior in the FLRW universe; see Eq. (G23) of [1]. C and G show a similar behavior to δ until the transition time, but after then their amplitudes decrease; see Eq. (G28) of [1].

In Fig. 10, we show the evolution of the decoupled gravitational wave perturbation for $S_\alpha = (0, -\sqrt{3}, \sqrt{3})$. As the initial condition we take the growing mode (g_2) in Eq. (22). As in the case of the coupled gravitational wave, the decoupled gravitational wave changes its slope at earlier time with increasing r. Also, this fact is consistent with the slope change in $k^2 k_2 k^3 k_3/\Delta^2$; see Fig. 2. In the FLRW limit, $\bar{G}$ becomes constant which coincides with the FLRW behavior. The behavior of $\bar{G}$ can be compared with the one of G presented in Fig. 3(c).

IV. DISCUSSION

In this paper we investigated the evolution of perturbations in the Bianchi type-I universe model filled by a radiation fluid. Using the asymptotic solutions derived in [2] as initial conditions, the evolutions of perturbations were numerically investigated while the background model experiences a transition from the early anisotropic phase to the later radiation-dominated isotropic phase. We considered the evolution in the comoving gauge condition.

We restricted our attention to the configuration of perturbations where the wave propagation vector lies in a plane of two principal axes of the background anisotropy. The perturbation equations can be categorized into two sets. In one set, the scalar mode and the tensor mode are

shown to be coupled each other. In the other set, we have a decoupled tensor mode which evolves freely from other modes. In both cases, the two separate vector modes work as source terms to the corresponding set.

In the shear-dominated stage, the temporal evolution of the perturbations depends on the background anisotropy. Near the transition time from the shear-dominated era into the radiation-dominated era, the perturbations change the growth rate. After then, the perturbations evolve like the ones in the FLRW universe.

In the numerical study we selected some combination of parameters out of the parameter space, which are (1) the background anisotropy, u, (2) the size of the perturbation characterized by the horizon crossing epoch of the given scale, η_H, (3) the direction of the wave propagation vector in a plane of two principal axes, r, and (4) the initial mode out of four $a_i(\mathbf{x})$'s in the comoving gauge or two $g_i(\mathbf{x})$'s for the decoupled gravitational wave. As the initial condition we mainly considered the a_3 mode (and the g_2 mode for the decoupled gravitational wave) which is one of two growing modes.

The assumptions used in this paper are the following: (1) radiation-filled Bianchi type-I model; (2) ignored the effect from the rotation mode; (3) plane wave perturbations; (4) wave vector which lies in a plane consisting of two principal axes of the background anisotropy; (5) numerical results in some selected parameter space of u, r, and η_H.

We show the effect of the parameter r on the evolution of perturbation. With increasing value of r, so that the wave vector of the perturbation is close to the $\hat{x}^2$ direction, the perturbation changes its growth rate at an earlier time. However, in the case of using the model in which the background is axisymmetric with respect to the $\hat{x}^1$ axis ($S_2 = S_3$), the behavior of the perturbation is independent of r.

Because of the nonvanishing shear in the background, the tensor mode is coupled with the scalar mode in the anisotropic stage. Thus, as the background evolution transits from the anisotropic to the isotropic stage, the resulting amplitude of the tensor perturbations viewed in the later isotropic stage should be related to the amplitude of scalar perturbations. We find that for the growing mode (a_3 mode) of initial conditions the tensor mode perturbation is comparable to the scalar mode perturbation for different values of the parameters r and u. The ratio of C to G is close to 1 for different r; see Fig. 3(d) for the background model with $S_\alpha = (0, -\sqrt{3}, \sqrt{3})$. The asymptotic solutions in the shear-dominated stage clearly show that for all four modes the amplitude of the G is linearly related to the one for C and δ; see Eqs. (19)–(21).

An accompanying case of the evolution of perturbations in a dust-filled Bianchi type-I background will be presented in a separate work.

ACKNOWLEDGMENTS

The author wishes to thank Dr. J. Hwang for helpful discussions and comments throughout the work.

APPENDIX: USEFUL COEFFICIENTS

We present some convenient expressions in the following. The following quantities appear often in our perturbation equations [Eqs. (14)–(18)]. We express the evolution of such quantities using the known exact solutions in the shear plus radiation stage. From the exact solutions in Sec. II A we can show

$$s'_\alpha = S_\alpha \frac{\eta_s}{\eta+\eta_s}, \quad \frac{\ddot{s}}{\dot{s}^2} = -\left(\frac{\eta_s}{\eta+\eta_s}\right)^2 - 2, \quad \frac{8\pi G\mu}{3\dot{s}^2} = \frac{\eta(\eta+2\eta_s)}{(\eta+\eta_s)^2}. \tag{A1}$$

The evolution of the wave vector follows from the equations in Sec. II B:

$$\bar{\Delta} = -\left(\frac{\eta}{\eta_H}\right)^2 \left(\frac{\eta_H+\eta_s}{\eta_H+2\eta_s}\right)^2 \left(\frac{\eta+2\eta_s}{\eta+\eta_s}\right)^2 \left(\frac{\eta}{\eta+2\eta_s}\right)^{-S_3} \left(\frac{\eta_H}{\eta_H+2\eta_s}\right)^{S_3} \frac{1+\left(\frac{\eta}{\eta+2\eta_s}\right)^{S_3-S_2} r^2}{1+\left(\frac{\eta_H}{\eta_H+2\eta_s}\right)^{S_3-S_2} r^2},$$

$$\frac{\Delta'}{\Delta} = -\frac{2\eta_s}{\eta+\eta_s} \frac{S_3 + S_2\left(\frac{\eta}{\eta+2\eta_s}\right)^{S_3-S_2} r^2}{1+\left(\frac{\eta}{\eta+2\eta_s}\right)^{S_3-S_2} r^2},$$

$$\frac{k^3 k_3}{\Delta} = -\frac{1}{1+\left(\frac{\eta}{\eta+2\eta_s}\right)^{S_3-S_2} r^2}, \qquad \frac{k^2 k_2}{\Delta} = -\frac{r^2}{\left(\frac{\eta}{\eta+2\eta_s}\right)^{S_2-S_3} + r^2}, \tag{A2}$$

where $r \equiv k_2/k_3$ and η_H is the value of η at the horizon crossing.

[1] H. Noh and J. Hwang, Phys. Rev. D **52**, 1970 (1995).
[2] H. Noh and J. Hwang, Phys. Rev. D **52**, 5643 (1995).
[3] J. Hwang, Astrophys. J. **415**, 486 (1993).
[4] M. Den, Prog. Theor. Phys. **79**, 1110 (1988).